

12063
Ilmenite Basalt
2426 grams

DRAFT



Figure 1: Sample 12063 with odd patch on surface. NASA S69-60610. Sample about 9 cm across.

Introduction

12063 is the largest sample and has the highest ilmenite content of the Apollo 12 basalts. It has been dated at 3.3 ± 0.1 b.y.

Bloch et al. (1971) found more micrometeorite craters on the top surface than the bottom for 12063. They found up to 50 craters per mm^2 surface area in the micron-size range.

This large sample was not identified in surface photography. It is believed to have been collected at Bench Crater together with 12039 (McGee et al. 1977). Knowledge of surface orientation is important and is

provided by the activity of ^{22}Na (Rancitelli et al. 1971). While 12063 had highest ^{22}Na activity on the top surface, it was found to have the highest ^{26}Al activity on the bottom, indicating that it had “turned over” in the past few hundred thousand years. Kirsten et al. (1971) used solar wind implanted He to show the “turnover” of 12063.

Petrography

McGee et al. (1977) describe 12063 as “a medium-grained porphyritic olivine, pyroxene basalt. Phenocrysts of rounded olivine (0.6 to 0.8 mm) and euhedral to subhedral pyroxene (0.3 to 1.5 mm) are set in a matrix of intergrown plagioclase, pyroxene and

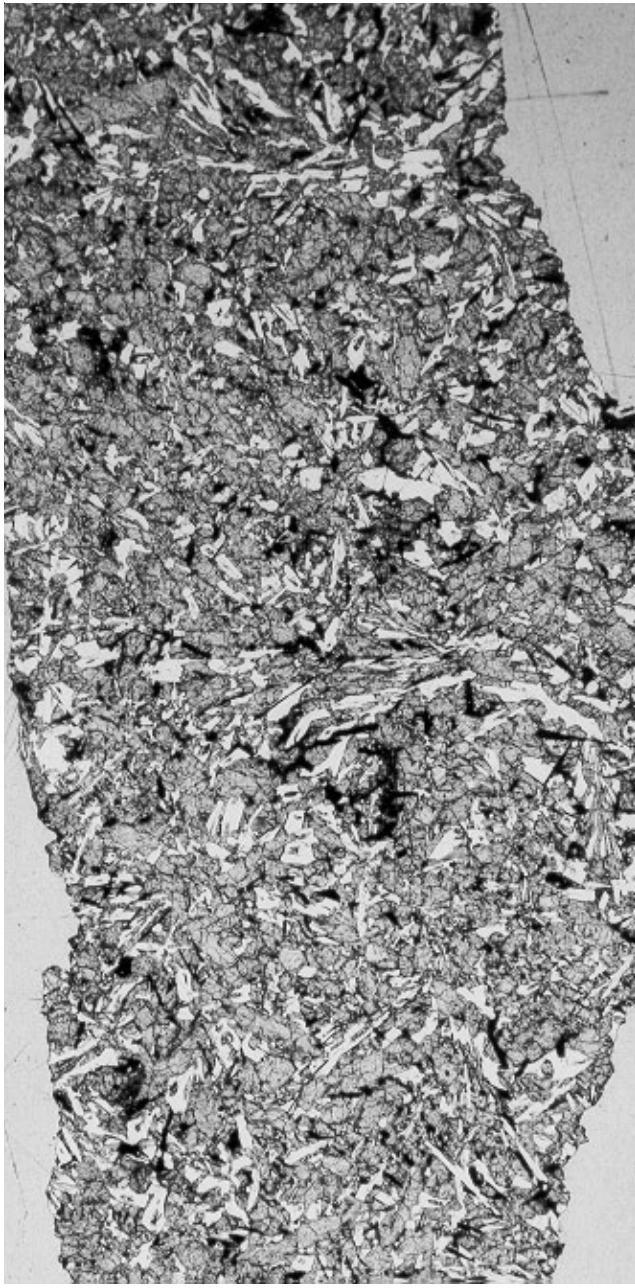


Figure 2: Transmitted light photomicrograph of portion of thin section 12063,15. NASA S70-31564. Length about 3 cm.

opaque minerals. Mesostasis fill interstices between matrix minerals and consists of vermicular, perhaps eutectic intergrowths, of single clinopyroxene crystals and glass.”

Taylor et al. (1971) described 12063 as a “microgabbro with subhedral olivine (Fo_{80}) enclosed by pale-pink pigeonite pyroxene which in turn zones outward to darker pink rims of augite. Pigeonite and augite ophitically enclose laths of polysynthetically twinned plagioclase (An_{90}). Small amounts of fayalite,

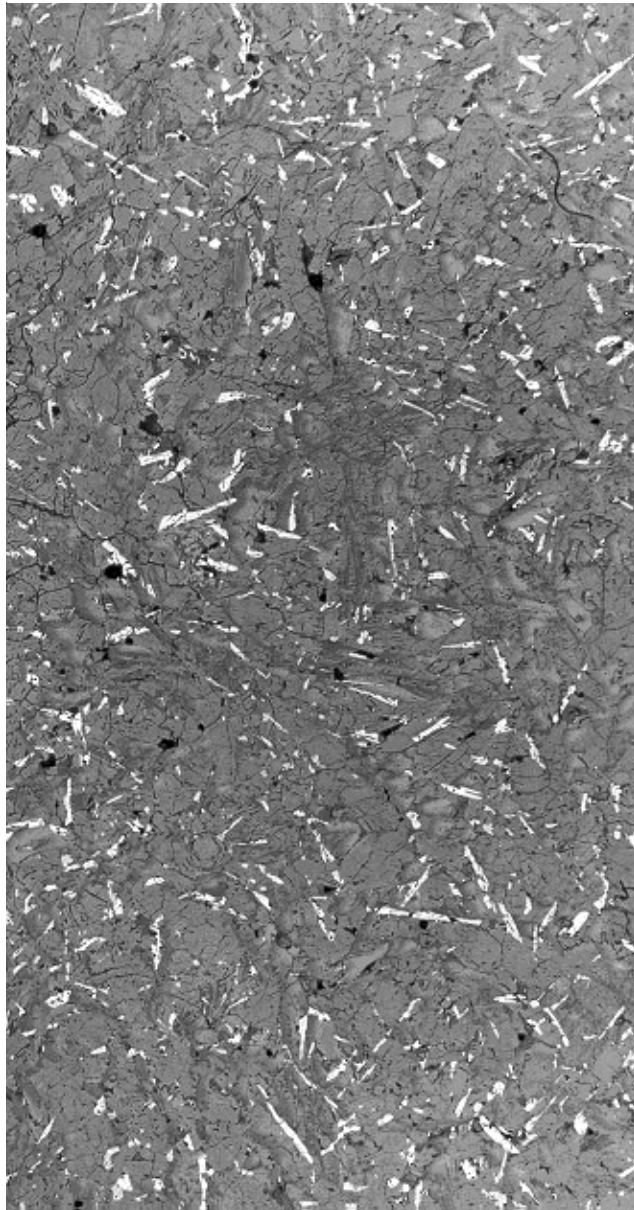


Figure 3: Reflected light photomicrograph of thin section 12063,14. NASA #S70-27960. Length about 3 cm.

cristobalite, and glass are associated in areas interstitial to pyroxene and plagioclase. The opaque minerals consist predominantly of ilmenite with lesser amounts of spinels, troilite, mackinawite (?), FeNi metal and metallic Cu.”

Mineralogy

Olivine: Carter et al. (1971) determined olivine in 12063 as Fo_{64-58} . Taylor et al. (1971) and El Goresy et al. (1971) studied the fine intergrowth of fayalite, glass and silica (cristobalite) found interstitial to the main minerals. Taylor et al. (1971) also reported olivine as magnesian as Fo_{80} ! (but this can't be right)

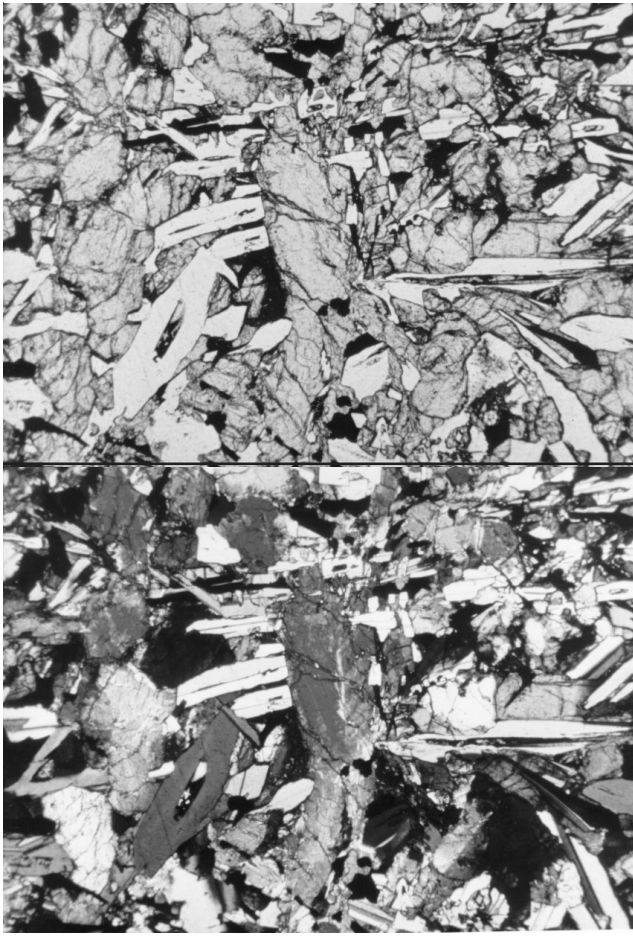


Figure 4: Photomicrographs of thin section 12063, 19 (plane-polarized light; crossed-nicols). NASA # S70-49543-49544. Scale 2.6 mm.

Pyroxene: The complex chemical zoning of pyroxene phenocrysts in 12063 was studied in detail by Hollister et al. (1971). McGee et al. (1977) reported the pyroxene compositions (figure 5).

Plagioclase: Plagioclase in 12063 began growth as hollow straws commonly inclosing Fe-rich pyroxene (Trzcienski and Kulick 1972).

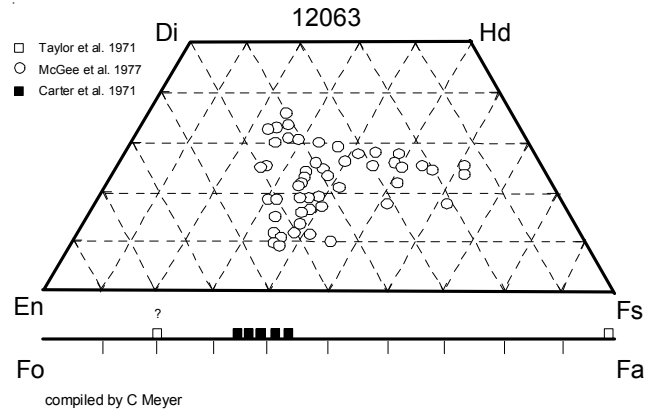


Figure 5: Pyroxene and olivine composition in 12063 (adapted from McGee et al. 1977, who adapted it from Hollister et al. 1971, Carter et al. 1971).

Ilmenite: McGee et al. (1977) describe ilmenite as blocky, irregular shaped bodies (0.1 to 0.3 mm). El Goresy et al. (1971) give an analysis. Arrhenius et al. (1971) determined the trace Zr content of ilmenite in 12063, noting that it was substantially higher than in terrestrial rocks.

Spinel: Cr-rich spinel with Ti-rich overgrowths occur as round octahedral inclusions in pyroxene. El Goresy et al. (1971) analyzed the spinels in 12063.

Potassium feldspar: Trzcienski and Kulick (1972) reported K-feldspar with up to 12.2% BaO in late-stage mesostasis.

Metal: Metallic iron occurs in troilite blebs and as small individual grains throughout (Taylor et al. 1971). It has 3 – 4 % Ni and ~ 1.5 % Co.

Mackinawite: (see Taylor et al. 1971, page 856) !

Chemistry

Willis et al. (1971), Wänke et al. (1971) and Wakita et al. (1971) determined the major elements, while Haskin

Mineralogical Mode of 12063

	McGee et al. 1977	Neal et al. 1994	Papike et al. 1976	Dungan and Brown 1977	Taylor et al. 1971
olivine	3-9	2.8	2.8	6	7.8
pyroxene	56-64	64.6	63.7	60	56.8
plagioclase	22-28	21.6	22.2	25	27.1
opaques	8		8.1	8	4.8
ilmenite		4.6			
chrom + usp		3.4			
“silica”		0.1	1.6	1.6	2
mesostasis	2-7	2.5	1.6	5	

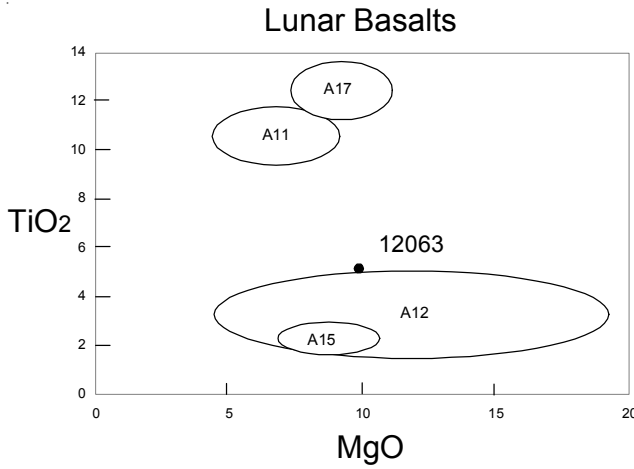


Figure 6: Composition of 12063 compared with that of other lunar basalts.

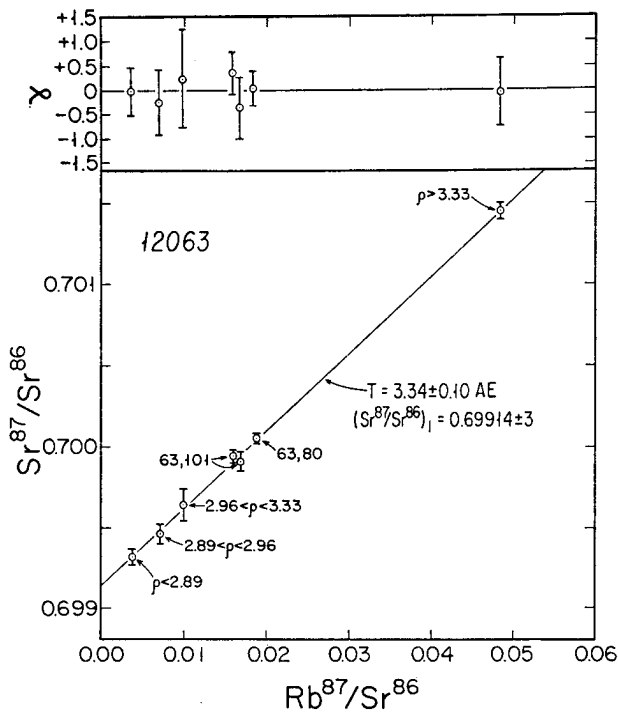


Figure 8: Rb/Sr isochron for 12063 (from Murthy et al 1971).

et al. (1971), Taylor et al. (1971), Baedecker et al. (1971) and Nyquist et al. (1979) reported the trace elements (figure 7). This sample has the highest TiO_2 content of the Apollo 12 basalts. Moore et al. (1971) reported 35 ppm carbon.

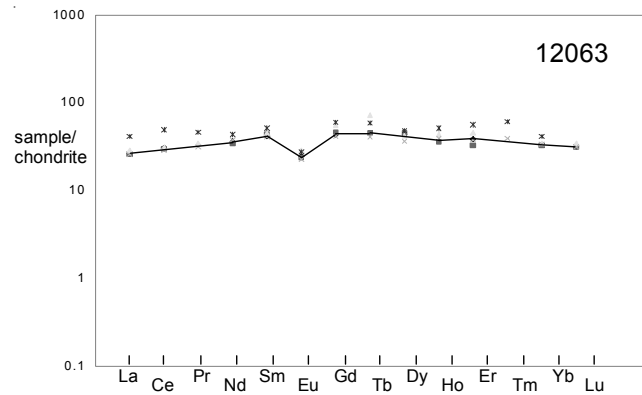


Figure 7: Normalized rare-earth-element diagram for basalt 12063 (superior data from Nyquist et al. 1979 connected).

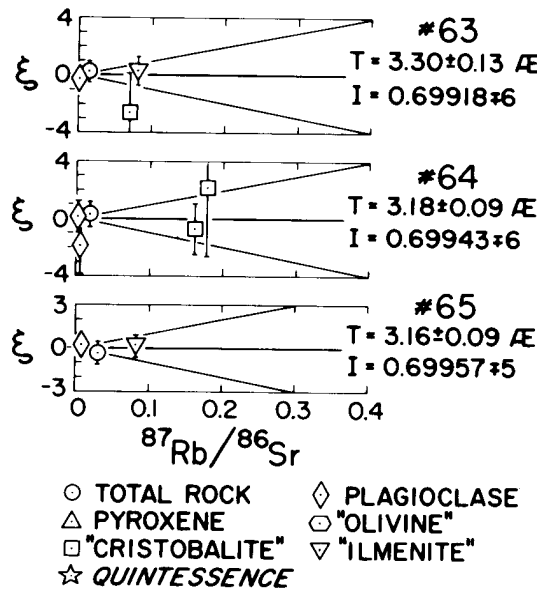


Figure 9: Rb/Sr isochron for 12063 (from Papanastassiou and Wasserburg 1971a).

Radiogenic age dating

Murthy et al. (1971) determined a Rb-Sr mineral isochron for 12063 (figure 8) with an age of 3.34 ± 0.1 b.y. Papanastassiou and Wasserburg (1971a) determined 3.30 ± 0.13 by Rb/Sr (figure 9). Cliff et al. (1971), Tatsumoto et al. (1971) and Silver (1971) attempted U/Pb age dating of this rock (without success!).

Summary of Age Data for 12063

Ar/Ar
Murthy et al. 1971
Papanastassiou and Wasserburg 1971a

Rb/Sr Nd/Sm
 3.34 ± 0.1 b.y.
 3.30 ± 0.13

Table 1a. Chemical composition of 12063.

reference	Murthy71	Willis71	Wanke71	Wakita71	Haskin71	Taylor71	Rancitelli71
weight				0.418 0.479			2426 g
SiO ₂ %	43.48	(b)	44.7 (d)	42.8 (d)			
TiO ₂	5	(b)	4.67 (d)	5 5 (d)			
Al ₂ O ₃	9.27	(b)	9.33 (d)	9.1 9.1 (d)			
FeO	21.26	(b)	21.48 (d)	21.2 (d)			
MnO	0.28	(b)	0.28 (d)	0.265 (d)			
MgO	9.56	(b)	8.37 (d)	11.4 (d)			
CaO	10.49	(b)	13 (d)	10.2 10.8 (d)			
Na ₂ O	0.31	(b)	0.29 (d)	0.275 0.279 (d)			
K ₂ O	0.063	0.061 (a)	0.061 (b)	0.076 (d) 0.064 (d)			0.066 (g)
P ₂ O ₅			0.14 (b)				
S %			0.09 (b)				
<i>sum</i>							
Sc ppm		55 (c)	62.9 (d)	55 (e)	60 (f)		
V		135 (c)	130 (d)	140 (e)	130 (f)		
Cr		3010 (b)	2580 (d)	2805 (d)	2500 (f)		
Co		36 (c)	39.1 (d)	46 (d)	40 (f)		
Ni		20 (b)	49 (d)		23 (f)		
Cu		8 (b)	12.9 (d)		5 (f)		
Zn		4.5 (b)					
Ga			5.3 (d)				
Ge ppb			100 (d)				
As			53 (d)				
Se							
Rb	0.96	0.902 (a)	0.8 (b)	1.1 (d) 0.4 (e)			
Sr	146	155 (a)	145 (b)	149 130 (d)		140 (f)	
Y		65 (b)	54.8		65 (f)		
Zr		133 (b)	128		140 (f)		
Nb		7.9 (b)	6.4		4 (f)		
Mo					0.04 (f)		
Ru							
Rh							
Pd ppb							
Ag ppb							
Cd ppb				18 (e)			
In ppb			2.3 (d)	3.4 (e)			
Sn ppb					120 (f)		
Sb ppb							
Te ppb							
Cs ppm			0.08 (d)	0.05 (e)	0.025 (f)		
Ba	66	64 (a)	67 (b)	140 (d) 60 (e)	60 (f)		
La			6.88 (d)	6 5.9 (e)	9.8 (f)		
Ce			19 (d)	17.5 (e)	30 (f)		
Pr			3.1 (d)	2.9 (e)	4.2 (f)		
Nd				17.1 (e)	20 (f)		
Sm			6.6 (d)	6.05 5.6 (e)	7.6 (f)		
Eu			1.62 (d)	1.3 1.43 (e)	1.6 (f)		
Gd			11 (d)	8.2 9.4 (e)	12 (f)		
Tb			2.65 (d)	1.5 1.66 (e)	2.2 (f)		
Dy			10.3 (d)	8.9 11.3 (e)	12 (f)		
Ho			2.46 (d)	2.24 2 (e)	2.9 (f)		
Er			7.35 (d)	6 5.3 (e)	9 (f)		
Tm				0.96 (e)	1.5 (f)		
Yb		5.7 (c)		5.71 (d) 5.6 5.4 (e)	6.8 (f)		
Lu				0.84 (d) 0.79 0.8 (e)	0.79 (d)		
Hf				6.3 (d) 3.6 (e)	5.4 (f)		
Ta			0.47 (d)				
W ppb			140 (d)				
Re ppb							
Os ppb							
Ir ppb			1.3 (d)				
Pt ppb							
Au ppb			2.9 (d)				
Th ppm			0.82 (d)	0.7 (e)	0.7 (f) 0.653 (g)		
U ppm			0.236 (d)		0.15 (f) 0.178 (g)		

technique: (a) IDMS, (b) XRF, (c) emission spec, (d) INAA, (e) RNAA, (f) SSMS, (g) radiation counting

Table 1b. Chemical composition of 12063.

reference	Tatsumoto71	Baedecker71	Nyquist79
weight			54 mg
SiO ₂ %			
TiO ₂			
Al ₂ O ₃			
FeO			
MnO			
MgO			
CaO			
Na ₂ O			
K ₂ O			0.0694 (h)
P ₂ O ₅			
S %			
sum			
Sc ppm			
V			
Cr			
Co			
Ni			
Cu			
Zn	2.3	(e)	
Ga	4.3	(e)	
Ge ppb			
As			
Se			
Rb			0.856 (h)
Sr			159 (h)
Y			
Zr			
Nb			
Mo			
Ru			
Rh			
Pd ppb			
Ag ppb			
Cd ppb	1.1	(e)	
In ppb	1.1	(e)	
Sn ppb			
Sb ppb			
Te ppb			
Cs ppm			
Ba		61.3	(h)
La		6.3	(h)
Ce		18.6	(h)
Pr			
Nd		16.5	(h)
Sm		6.14	(h)
Eu		1.41	(h)
Gd		8.55	(h)
Tb			
Dy		10.6	(h)
Ho			
Er		6.21	(h)
Tm			
Yb		5.38	(h)
Lu		0.772	(h)
Hf			
Ta			
W ppb			
Re ppb			
Os ppb			
Ir ppb		<0.04	(e)
Pt ppb			
Au ppb			
Th ppm	0.679	0.637	(a)
U ppm	0.191	0.191	(a)

technique: (a) IDMS, (b) XRF, (c) emission spec, (d) INAA, (e) RNAA, (h) IDMS

Cosmogenic isotopes and exposure ages

Rancitelli et al. (1971) determined the cosmic ray induced activity of ²²Na = 38 dpm/kg, ²⁶Al = 78 dpm/kg, ⁴⁶Sc = 6 dpm/kg, ⁴⁸V = 19 dpm/kg, ⁵⁴Mn = 37 dpm/kg and ⁵⁶Co = 30 dpm/kg. The highest ²²Na was on this top, while the highest ²⁶Al was on the bottom surface of this rock. Burnett et al. (1975) determined an exposure age of 140 ± 40 m.y. and Marti and Lugmair (1971) determined an exposure age of 95 ± 5 m.y. by ⁸¹Kr/⁸³Kr. Hintenberger et al. (1971) determined exposure ages for 12063 using ³He (65 m.y.), ²¹Ne (69 m.y.) and ³⁸Ar (72 m.y.). Kirsten et al. (1971) used solar wind implanted He to show turnover of 12063.

Other Studies

Herzenberg et al. (1971) determined Mössbauer spectra for pyroxene in 12063. Adams and McCord (1971) measured the spectral reflectivity of 12063 and its mineral components (figure 12).

Hargraves and Dorety (1971) and Pearce et al. (1971) reported studies on the magnetic properties of 12063, finding that the magnetic remanence was weak.

Hoyt et al. (1971) studied the thermoluminescence for the top, bottom and middle of 12063 (figure 11) and found the highest TL was on the top surface. Crozaz et al. (1971) studied tracks and micrometeorite pits on 12063. They determined the track density vs. depth (figure 10).

List of Photo #s for 12063

S69-60600 – 60620	B & W mug
S69-61664	
S69-60597 – 60598	
S70-28675	
S70-28680	
S70-49534 – 535	
S70-49537 – 540	
S70-49543 – 545	
S70-49847 – 849	
S70-49888	
S49-50557 – 558	
S70-31564	TS
S70-27960	TS reflected
S70-39837 – 837	processing
S79-27081 – 083	

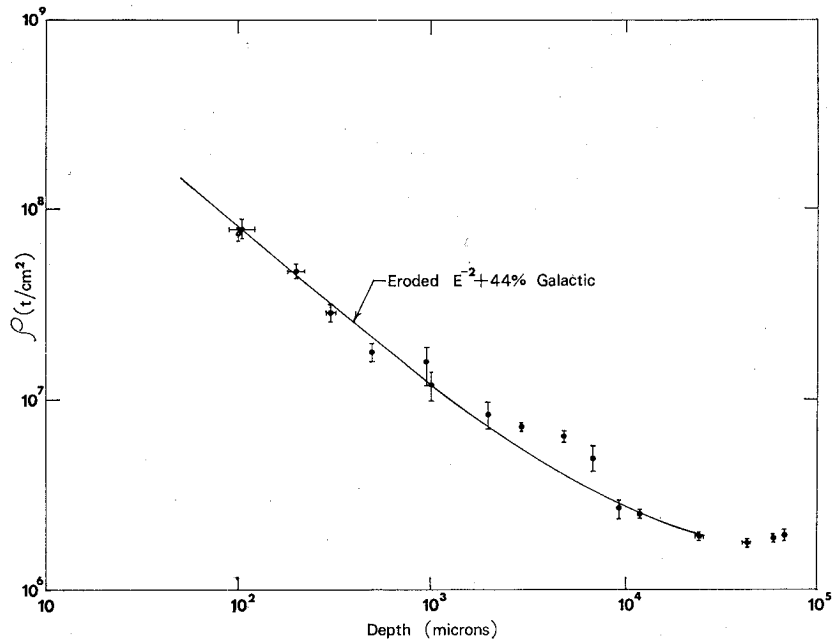


Figure 10: Track density vs. depth in a vertical section of 12063 (from Crozaz et al. 1971).

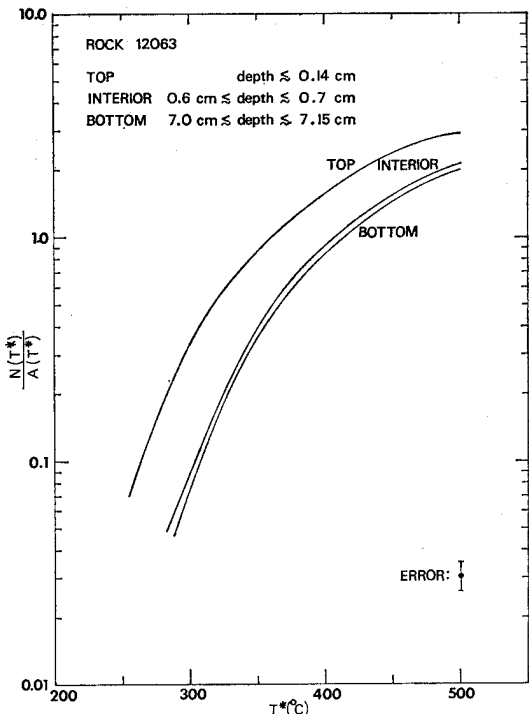


Figure 11: Thermoluminescence curves for samples 12063 (from Hoyt et al. 1971).

Bogard et al. (1971) and Funkhouser et al. (1971) reported the content and isotopic composition of rare gases in 12063. Clayton et al. (1971) reported oxygen isotopic analysis of mineral separates.

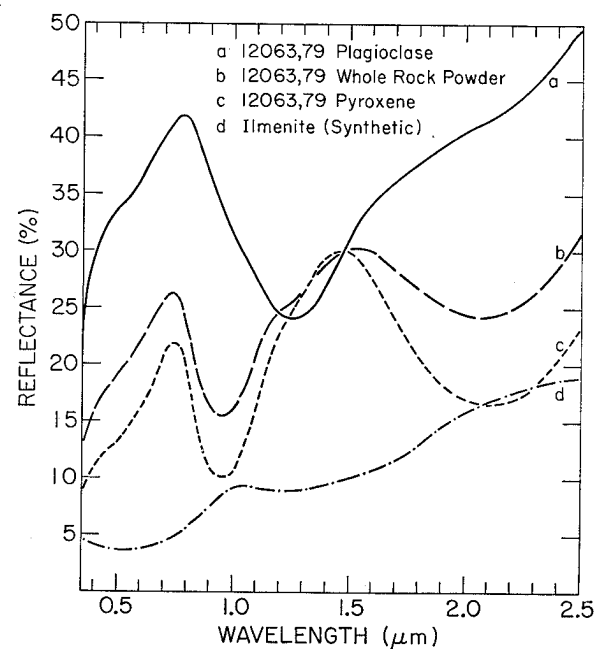


Figure 12: Spectral reflectivity of 12063 powder and plagioclase and pyroxene mineral separates (from Adams and McCord 1971).

Processing

A slab was cut through the middle of 12063 (figure 14) and two columns (,31 and ,33) were cut from the slab (figure 17). The details of the columns are shown in figures 18 and 19.



Figure 13: Photo of 12063 showing zap pits. Sample is about 12 cm long. NASA # S69-60606.

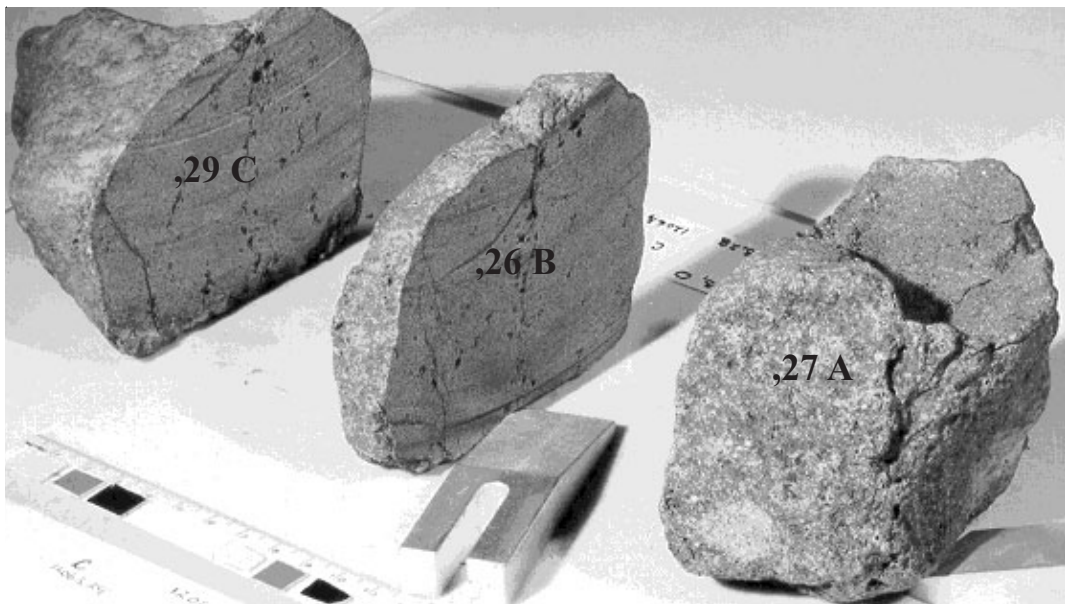
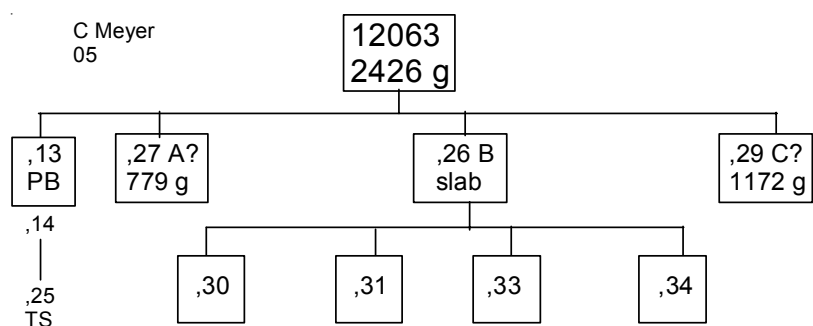


Figure 14: Group photo of 12063 after slab cut in 1970. NASA S70-39862. Scale in cm.
Slab about 1 cm thick.



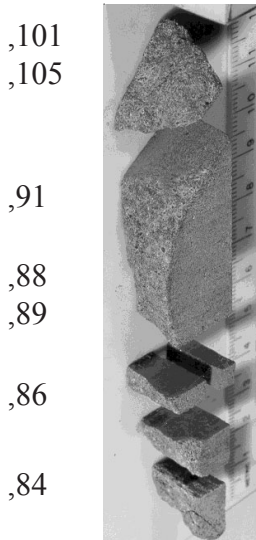
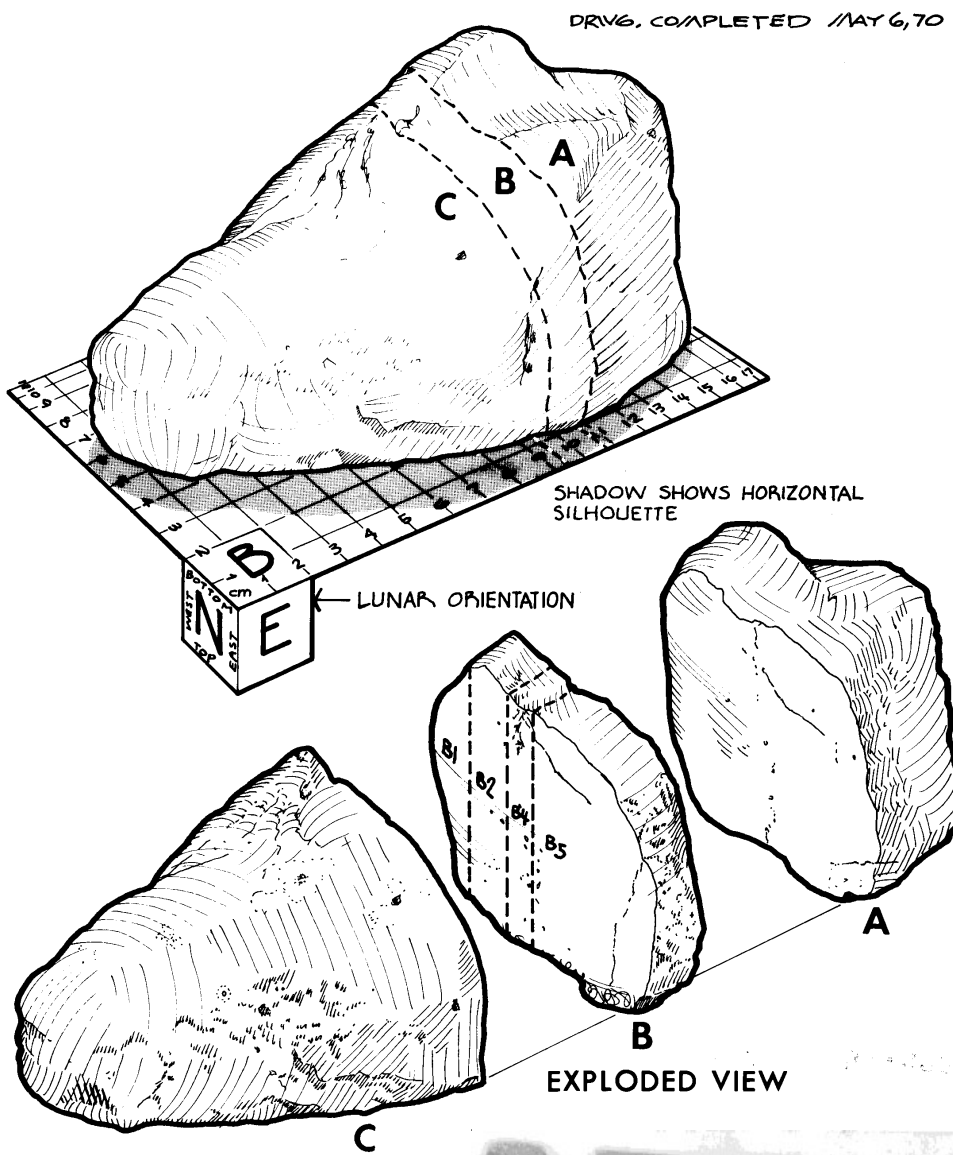


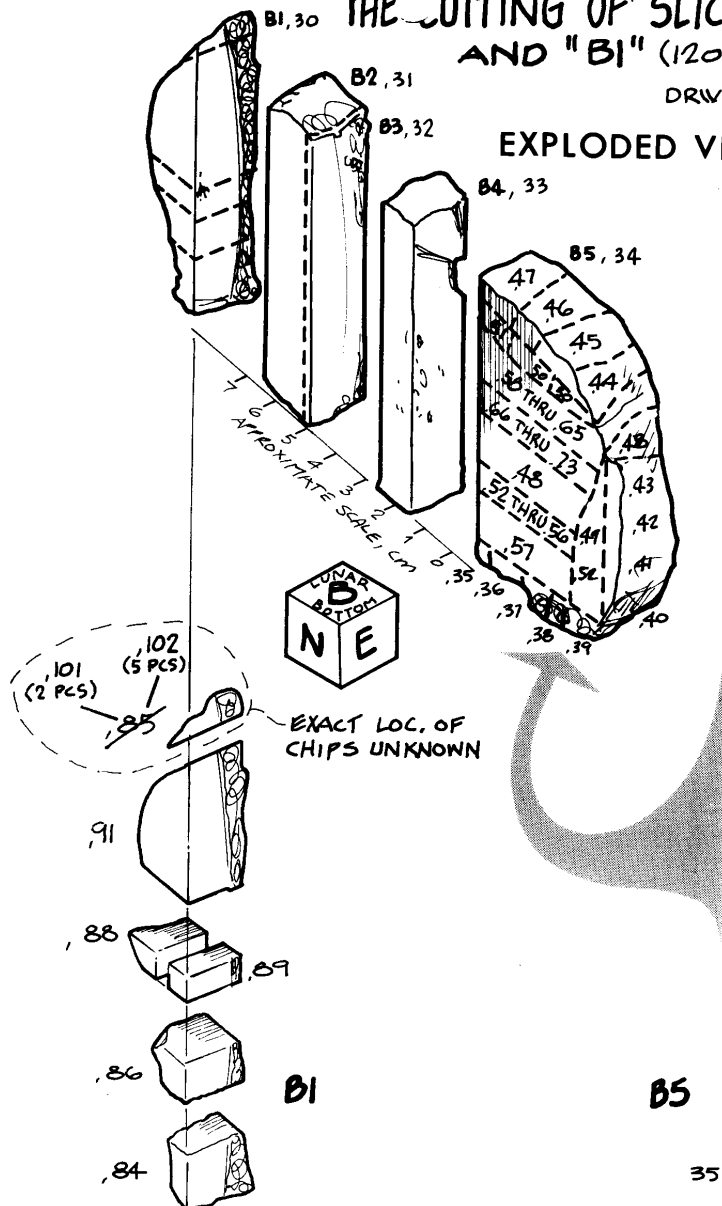
Figure 15: Group photo of pieces cut from end piece of slab 12063,30. NASA S70-39844.

Figure 16: Pieces cut from 12063,34 end of slab. Bigfoot and toes. NASA #S70-39837.

THE CUTTING OF SLICE "B" (12063, 28) AND "B1" (12063, 30)

DRIVE COMPLETED MAY 7, 70

EXPLODED VIEW



THE CHIPPING OF "B5" (12063, 34)

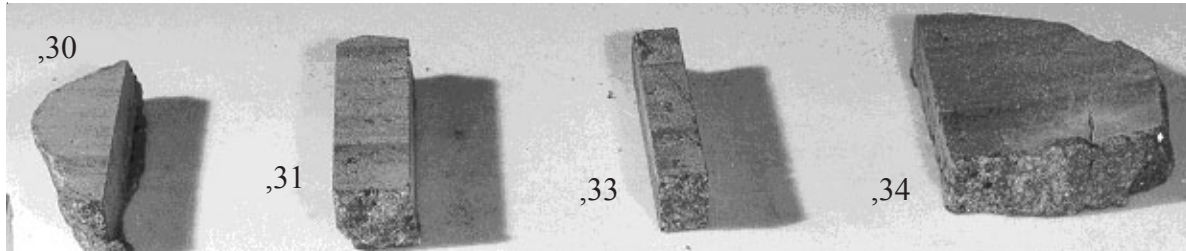
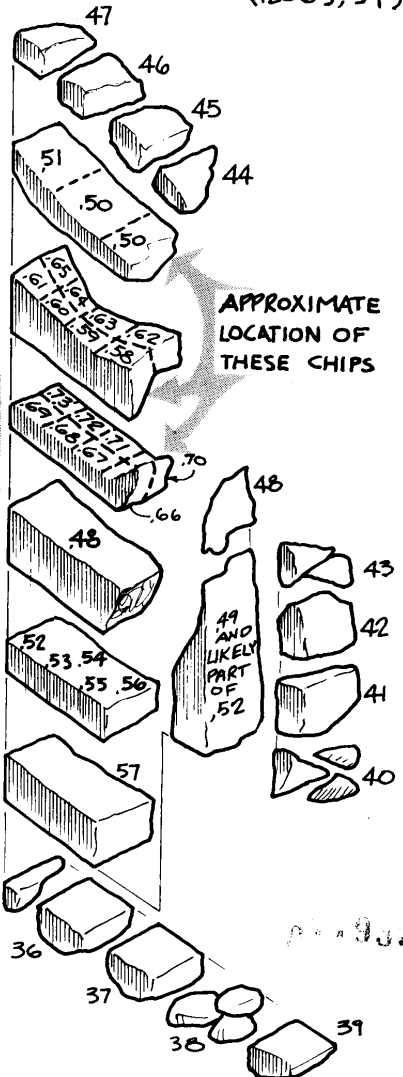
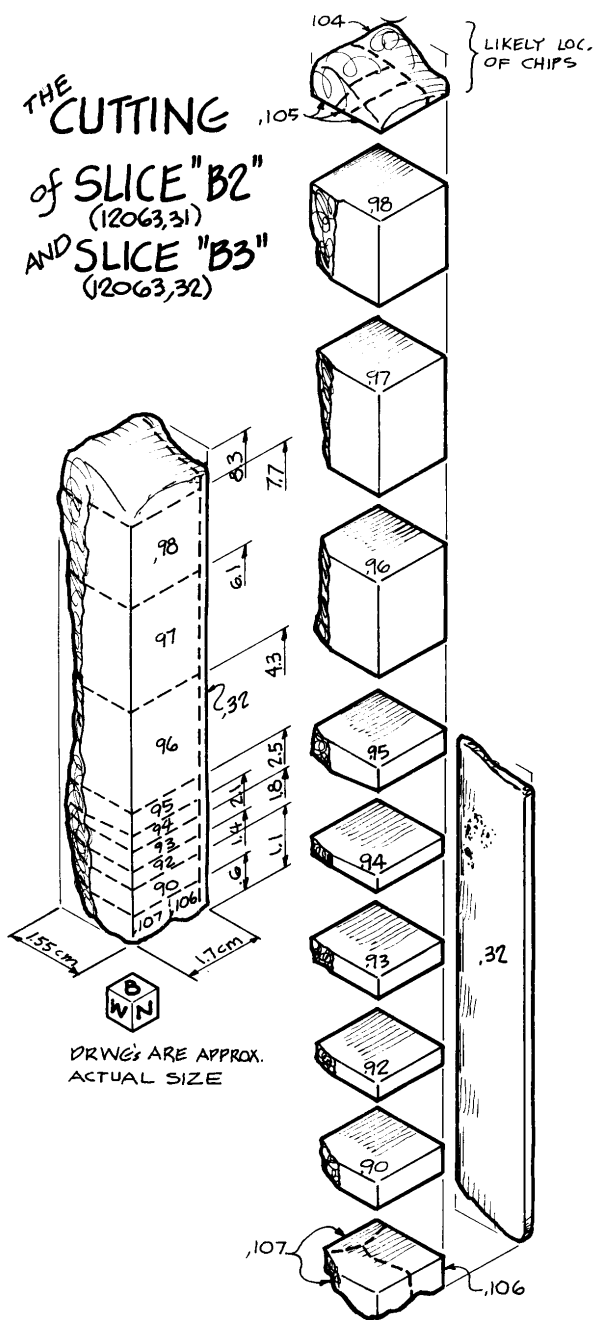


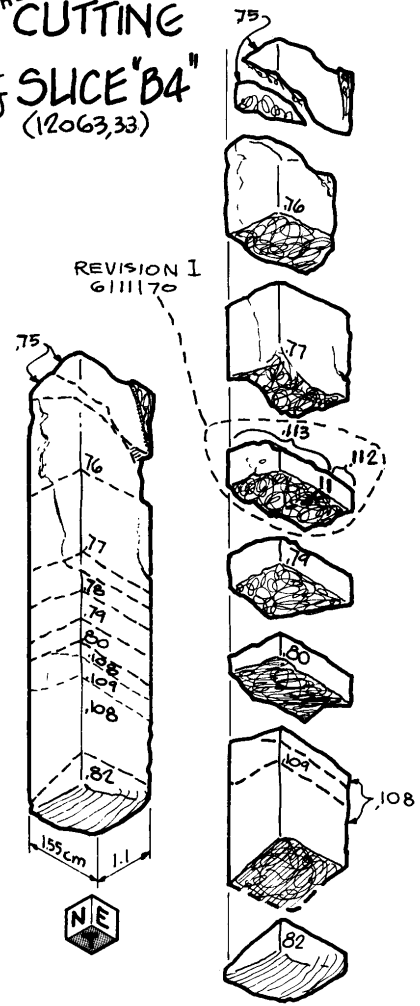
Figure 17: Group photo of columns cut from slab 12063,28. NASA S70-39857.

THE CUTTING
of SLICE "B2"
(12063,31)
AND SLICE "B3"
(12063,32)



DRWG. CO. COMPLETED MAY 7, 70
REV. I JUNE 11, 70

THE CUTTING
of SLICE "B4"
(12063,33)



DRWG FINISHED MAY 7, 70

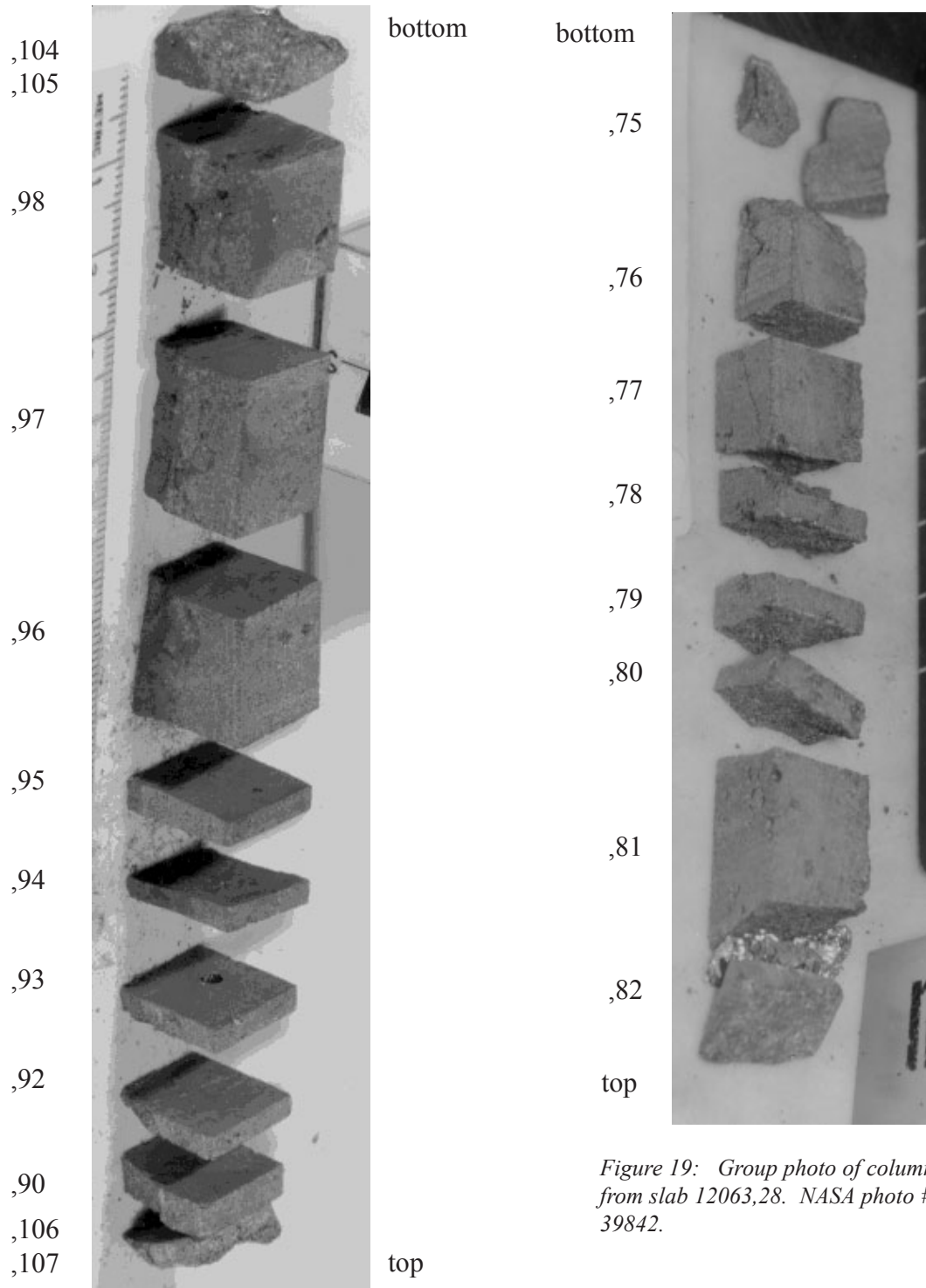


Figure 18: Group photo of column (.31) cut from slab (12063,28). Cubes are about 1.5 cm. NASA # S70-39848.

Figure 19: Group photo of column (.33) cut from slab 12063,28. NASA photo # S70-39842.